VI International Conference on Adaptive Modeling and Simulation
ADMOS 2013
J. P. Moitinho de Almeida, P. Díez, C. Tiago and N. Parés (Eds)

A NEW RESIDUAL LEAST SQUARES ERROR ESTIMATOR FOR FINITE VOLUME METHODS – APPLICATIONS TO LAMINAR FLOWS

Duarte M. S. Albuquerque*, José M. C. Pereira* and José C. F. Pereira*

*Instituto Superior Técnico (IST), IDMEC, LASEF
Universidade Técnica de Lisboa
Av. Rovisco Pais, 1, 1049-001, Lisbon, Portugal
e-mail: duartealbuquerque@ist.utl.pt, webpage: http://www.lasef.ist.utl.pt/

Key words: *h*-refinement, *a-posteriori* error estimation, Finite-Volume, incompressible flow, unstructured grids, least squares reconstruction

Abstract. Adaptive refinement is an important technique to reduce the computation time of flows in very refined meshes and increasing the local accuracy of the simulation.

A new *a-posteriori* error estimator, suitable for h-adaptive methods on unstructured grids, is based on the residual evaluation and a high-order polynomial reconstruction. The results are performed by the authors own Navier-Stokes code, which has been used to solve different adaptive problems [1, 2, 3].

The residual least squares (RLS) estimator is applied to different problems with a known analytic solution to study the numerical error decay with the adaptive algorithm and it is compared with the classic Taylor Series estimator [4, 5]. The proposed adaptive procedure is also applied to 3D flows around a sphere for two different types of grids.

The main goal of the present study is to perform the mesh refinement maintaining the global spatial accuracy to a desired level in the overall computational domain.

1 INTRODUCTION

The reduction of mesh generation effort and the computing time are of outmost relevance for CFD simulations of engineering fluid flow applications. Adaptive techniques reduce the time of the unstructured mesh generation and potencially the computing time, because the adaptive mesh has a smaller number of cells than the equivalent uniform mesh. Adaptive mesh refinement requires an estimator that shows the error distribution to refine locally the mesh. The information from the error estimator and the stop criterion should embody numerical accuracy and physical contrains of the numerical solution.

From the point of view of Finite Element Methods FEM the error estimators are well established and can be divided in three major groups: gradient recovery estimators,

explicit and implicit residual error estimates. A summary of different error estimators used in context of FEM was done by several authors [6, 7, 8, 9].

The Richardson Extrapolation [10] is the most popular error estimator in the finite-volume method (FVM) context and requires the solutions on two meshes with different spacings, which can be difficult to obtain in 3D industrial flow configurations. There are some attempts of single-mesh error estimators, based on energy conservation and angular moment conservation equations, see Haworth *et al.* [11]. Error estimators based on high order face interpolation was proposed by Muzaferija and Gosman [12] and later, Jasak and Gosman [4, 5] proposed an error estimator based in the Taylor series truncation error and another one based in the conservation of the second moment of the solution. Yahia *et al.* [13] has applied the Taylor series truncation to edges integral in the framework of r-adaptivity. Error estimator based on the residual error from the governing equations was investigated by Jasak and Gosman [14] and Juretic [15] extended it to a face based error estimator.

The Residual Least Squares error estimator has two main advantages, when compared to another approaches: the polynomial reconstruction made with the Least Squares method has the versatility required to be used in the case of unstructured grids which can have an arbitrary cell distribution and the Residual re-evaluation has information from the governing equations and the grid quality.

The adaptive grids are treated as unstructured grids, so the same convective and diffusive schemes are used, garantee second order error decay between the cells with different levels of refinement. In addition the new decision algorithm uses the computed information from error estimators without requiring any input parameter from the user or any previous knowledge of the numerical solution.

2 NUMERICAL METHOD

2.1 Governing Equations and Unstructured Grids Formulation

The steady isothermal flow of an incompressible fluid is governed by the mass and momentum conservation laws, being expressed by the incompressibility constraint and the Navier-Stokes equations:

$$\nabla \cdot \mathbf{u} = 0 \tag{1}$$

$$\nabla \cdot (\mathbf{u} \otimes \mathbf{u}) = \nabla \cdot \left(\nu \nabla \mathbf{u} + \nu \nabla^T \mathbf{u}\right) - \frac{1}{\rho} \nabla p \tag{2}$$

where $\mathbf{u}$ is the velocity vector, ν is the kinematic viscosity, ρ is the fluid's density and p is the fluid's pressure. The governing equations are discretized on unstructured meshes made of cells of arbitrary topology, to address the multiple faces that arise in interfaces between refined and non-refined cells. Each cell P is a polyhedron with a closed boundary ∂P which is composed by a variable number of faces $\partial P = \{S_1, S_2, ..., S_F\}$. Each face S_k is a plane polygon of arbitrary orientation which connects P and it's neighbour cell P_k,

see Figure 1. The computational points are located at the centers of each control volume corresponding to the so-called "collocated" or "non-staggered" arrangement.

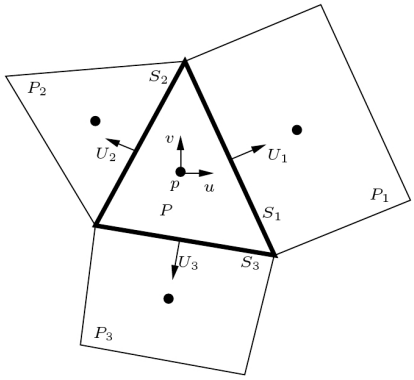

Figure 1: General 2D Polyhedral Control Volume

2.2 Pressure Velocity Coupling Algorithm

The SIMPLE algorithm [16] is used for the pressure velocity coupling. The SIMPLE algorithm starts by computing an approximate velocity field $\mathbf{u}^*$, which satisfies the momentum equations using the values from the previous iteration n. The steady equation is solved implicitly and linearization of the convection contribution is required:

$$\sum_{f=1}^{F} U_f^n \mathbf{u}_f^* - \nu \sum_{f=1}^{F} (\nabla \mathbf{u}^*)_f . \mathbf{S}_f = -\frac{V_P}{\rho} \nabla p^n \tag{3}$$

where U_f^n is the face velocity defined by $\mathbf{u}_f^n . \mathbf{S}_f$, $\mathbf{S}_f$ is the face surface vector defined by $S_f \mathbf{n}_f$, $\mathbf{n}_f$ is the normal unit vector of the face f and V_P denotes the cell P volume. A system of linear equations is assembled in this form:

$$\frac{1}{\alpha_u} a_p \mathbf{u}_p^* + \sum_{l=1}^{F} a_l \mathbf{u}_l^* = -\frac{V_P}{\rho} \nabla p^n + \frac{1-\alpha_u}{\alpha_u} a_p \mathbf{u}_p^n \tag{4}$$

being α_u the under relaxation factor for the momentum equations. The face velocity U_f^* is computed with Rhie-Chow interpolation [17]:

$$U_f^* = \overline{\mathbf{u}_p^*} . \mathbf{S}_f - \overline{\frac{\alpha_u V_P}{\rho \, a_p}} ((\nabla p^n)_f - \overline{(\nabla p^n)}) . \mathbf{S}_f \tag{5}$$

where the over-lined values are obtained by interpolation from the two cells which have the same face f and a_p are the momentum system matrix's main diagonal elements. This

face velocity is used to solve the pressure correction equation:

$$\sum_{f=1}^{F} \overline{\frac{\alpha_u V_P}{\rho\, a_p}} (\nabla p')_f . \mathbf{S}_f = \sum_{f=1}^{F} U_f^* \tag{6}$$

where p' is the pressure correction. After solving the Poisson equation 6, the velocity values are corrected with the p' new values to satisfy the continuity equation 1. The conservative face velocity is computed by:

$$U_f^{n+1} = U_f^* - \overline{\frac{\alpha_u V_P}{\rho\, a_p}} (\nabla p')_f . \mathbf{S}_f \tag{7}$$

the cell velocity is corrected by:

$$\mathbf{u}^{n+1} = \mathbf{u}^* - \overline{\frac{\alpha_u V_P}{\rho\, a_p}} (\nabla p') \tag{8}$$

and the pressure is updated:

$$p^{n+1} = p^n + \alpha_p p' \tag{9}$$

the SIMPLE algorithm requires an under relaxation factor for pressure α_p. From this point the residuals are computed, If they are lower than a prescribed value the cycle ends, if not the computation advances to the next iteration, back to equation 4.

2.3 Numerical Schemes

The author's own code SOL has the capability to make different types of regressions from the discrete cell values by solving a Weighted Least Squares (WLS) problem. Different types of polynomials and cell sets can be used in these regressions. Figure 2 shows examples of cell sets composed by different types of cell neigbours. The subfigure 2(a) shows the first and second cell's neighbours by face in a cartesian grid and the subfigure 2(b) shows the first and second cell's neighbours by vertex in a grid made by triangles.

The versatility of the regressions is suitable to compute the diffusive and convective values of the arbitrary unstructured cells and achieve second order accuracy, see Kobayashi *et al.* [18, 19] for details. Since the face regressions are centered in the face centroid, they can deal with the severe orthogonality and skewness deviations which exist in the interfaces between refined and non-refined cells, increasing the accuracy of the diffusive and convective schemes.

All the least squares regressions use a weight function W_P, given by the inverse square of the distance:

$$w_P = |x_P - x_{ref}|^{-2} \tag{10}$$

where x_P is the cell P centroid coordinates and x_{ref} is the coordinates of the regression reference.

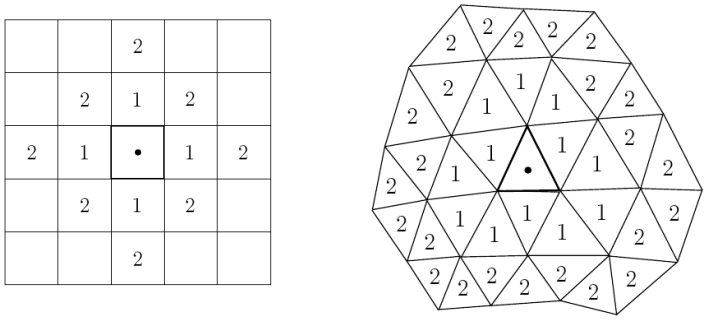

(a) Cell Neibours by Face (b) Cell Neibours by Vertex

Figure 2: Different Examples of Cell Neibours

Both diffusive and convective values are computed with a single regression, using a linear polynomial and the various cells that have the face's vertices. Figure 3 shows examples of different computational molecules used in the numerical schemes. Where the cells used for each regression k of the face S_k are marked with the respective number k.

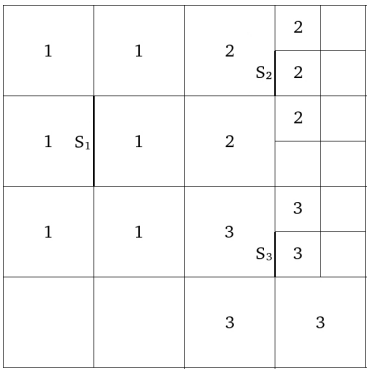

Figure 3: Possible Stencils used in the Convective and Diffusive Terms Computation

To achieve the second order integration with the finite volume method the regression is centred at the face's centroid.

The convective and diffusive schemes used in this work may originate a non positive definite matrices, so a deferred correction approach (Ferziger [20]) was used where a stable scheme is computed implicitly and the least squares scheme is computed explicitly. As stable schemes, the central differences scheme is used for the diffusive term and the convective fluxes are approximated by the first order upwind.

3 ADAPTIVE ALGORITHM AND ERROR ESTIMATORS

3.1 Adaptive Algorithm

Error estimators are required for the adaptive decision algorithm and they give a good approximation of the numerical error and its distribution in the computational domain. With this information is possible to compute an estimation of the ideal hydraulic radius h_i distribution for a desired local error E_0. For a second order method in space, the following equations are valid:

$$|E| \sim Kh^2 \tag{11}$$

$$|E_0| \sim Kh_i^2 \tag{12}$$

where E is the error estimation and K is an unknown constant. After some algebraic manipulation:

$$h_i \sim h\sqrt{E_0/E} \tag{13}$$

Ideally, the formula 13 can be used to create adaptive grids with approximately constant error if combined with an automatic grid generator.

The adaptive procedure used in this work is based in the maximum value of the error estimator. The cells with an error higher than $\lambda\ max(|E|)$ are selected for h-refinement, where λ is a factor that depends of the method's order. In the case of second order method this value λ is equal to 0.25, which is the reduction factor $(h_L/h_{L+1})^2$ of the local error, in each grid refinement.

3.2 Taylor series truncation error

The Taylor series error estimator [4] is derived by the 2^{nd} order term of the Taylor series and it is computed by:

$$E_T = \frac{1}{2V_P}\left|\left(\frac{\partial^2\phi}{\partial x_i \partial x_j}\right)_P\right|(M_{ij})_P \tag{14}$$

where $(M_{ij})_P$ is the inertia tensor of the cell P. The Hessian matrix values are computed from a regression made with a 2^{nd} order polynomial from the cell's first and second neighbours. Due to the assumption of linear variation inside the computational cells, zones with lower errors will have lower values of the Hessian matrix.

3.3 Residual Least Squares

A regression is done with a 3^{rd} order polynomial and considering the cell's first and second neighbors. New face's values and gradients are computed and compared with the values from the convection and diffusion schemes. One way to do this, is by recomputing new residual values, which indicate if the values satisfies the governing equations. The Residual Least Squares (RLS) vector is computed for each cell by the following formula:

$$\mathbf{E}_R = \frac{\sum_{f=1}^{F} U_f^n \mathbf{u}_f - \nu \sum_{f=1}^{F} (\nabla \mathbf{u})_f . \mathbf{S}_f + \dfrac{V_P}{\rho} \nabla p^n}{a_p} \tag{15}$$

where the values $\mathbf{u}_f$ and $(\nabla \mathbf{u})_f$ are computed from the 3^{rd} order polynomial, a_p is the matrix value used for the momentum equations, which is required to give the RLS error the same dimensions of the dependent variable. This error gives the indication for local refinement if the differences between 3^{rd} order profile and the numerical discretization affect the governing equations. Unlike the Taylor series the RLS criteria depends on the governing equations discretization and the grid quality.

4 RESULTS

4.1 Poisson Equation in a L-Shaped Domain

For this test case the Poisson equation $\nabla^2 \phi = 0.0$ was solved in a L-shaped domain $[-1,1]^2 \setminus ([0,1] \times [-1,0])$ Dirichlet boundary condition is prescribed in all boundaries and the analytic solution is given by the following equation:

$$\phi(x,y) = r^{2/3} sin(2\varphi/3) \quad with \;\; (x,y) = r(cos\,\varphi, sin\,\varphi) \tag{16}$$

The computations started with a grid of 12 triangles, three types of refinement are applied to this grid: one with uniform refinement and other two with the adaptive procedure using the classic Taylor series or the RLS as error estimators. The goal is to study the main differences between the two error estimators and evaluate their effectiveness. Figure 4 shows the mean and maximum error for the three types of grids, after 15 levels of refinement for the Taylor series and 22 levels of refinement for the RLS errors estimators:

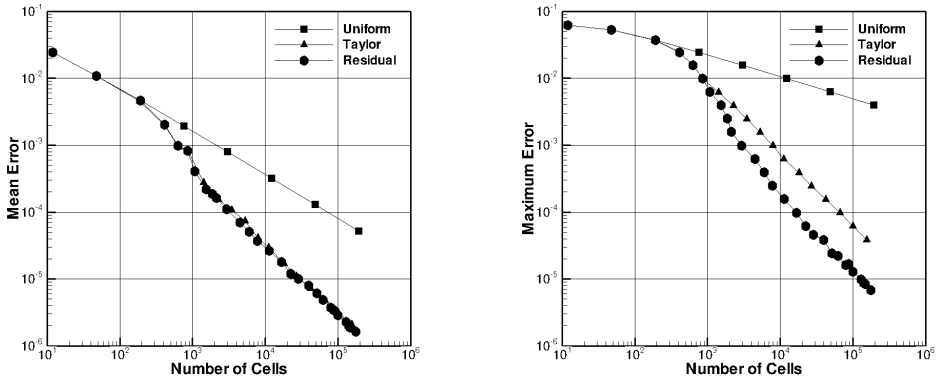

(a) Mean Error over Number of Cells (b) Maximum Error over Number of Cells

Figure 4: Poisson Equation: Mean and Maximum Error for the Uniform and Adaptive Grids

For the uniform grid case, the mean and maximum error slope has an order of 4/3 and 2/3, respectively. Although, at the singularity point $(x, y) = (0, 0)$ the analytic solution is zero, the analytic gradient is infinite which causes the method to have an order accuracy lower than 2 for uniform grids.

For both error estimators, the mean error of the adaptive grids has second order slope, due to the difference between the slopes of the adaptive and uniform grids, the mean error from the adaptive grids is much lower than the mean error from the uniform grid.

In the subfigure 4(b), the maximum error for the three types of grids is shown. The adaptive grid with the TS estimator has an maximum error 100 times lower than the error of the uniform grid and the adaptive grid with the RLS estimator shows an maximum error 1000 times lower, showing an improvement when compared with TS estimator. The ratio between the maximum and mean error, which is a measurement of adaptivity efficiency, is 0.053 for the TS estimator and 0.2336 for the RLS estimator.

Figure 5 shows the final adaptive grids obtained with the TS and RLS error estimators. The adaptive grid with TS has more refined cells and a circular pattern in the grid interface, this happens due to the loss of accuracy of the TS error estimator after some adaptive levels. The adaptive grid with RLS has a lower number of cells and a rectangular pattern is observed, there is an increase in the error estimator accuracy as it was observed in the subfigure 4(b), there is an over estimation of the numerical error in the boundaries of the computational domain.

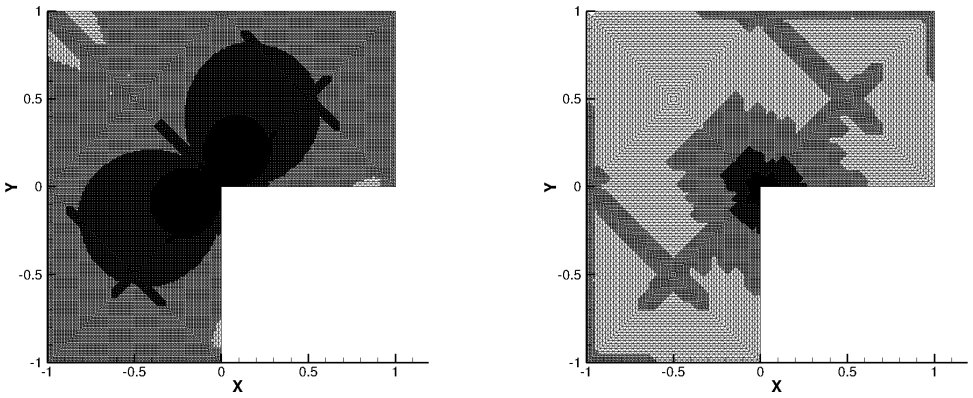

(a) Adaptive Grid using the Taylor Estimator (b) Adaptive Grid using the RLS Estimator

Figure 5: Poisson Equation: Adaptive Grids for the Taylor and RLS Estimators

4.2 Convection-Diffusion Equation - Point Source in Cross-Flow

For this test case, the convection-diffusion equation $U\dfrac{\partial\phi}{\partial x} = \Gamma\nabla^2\phi$ is solved. The selected analytical solution was used in previous works by Jasak and Gosman [4, 5] and is defined by:

$$\phi(x,y) = \frac{S}{2\pi\Gamma}K_0(\frac{U\sqrt{x^2+y^2}}{2\Gamma})e^{(0.5xU/\Gamma)} \tag{17}$$

where $S = 16.67\,[\phi/s]$ is the source magnitude, $\Gamma = 0.05\,[m^2/s]$ is the diffusion coefficient, $U = 1.0\,[m/s]$ is the imposed velocity in the x axis and K_0 is the modified Bessel function of the second kind and zero order.

This problem is solved in a rectangular domain $[0.0, 4.0] \times [-0.5, 0.5]$, the line-source is located at $0.05\,m$ of the left boundary to avoid numerical problems from this singularity. Dirichlet boundary conditions are prescribed in all boundaries, except for the right boundary ($x = 4.0$), where a null gradient is imposed.

The same refinement test were done for this solution, a Cartesian grid of 16×4 is used as initial grid and the adaptive algorithm is used until 20 levels of refinement are reached. The mean and maximum error, for the uniform and adaptive grids are shown in figure 6.

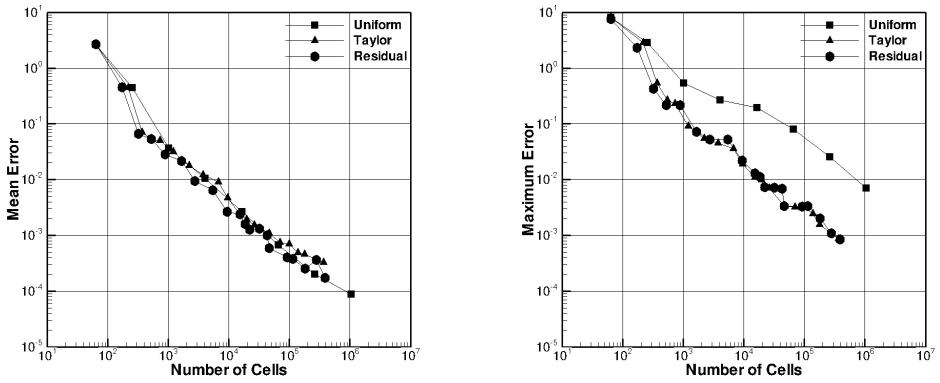

(a) Mean Error over Number of Cells (b) Maximum Error over Number of Cells

Figure 6: Line Source: Mean and Maximum Error for Uniform and Adaptive Grids

The curves of the mean error (subfigure 6(a)) show the same slope for the three grids, the adaptive grids doesn't show any improvement in the mean error when compared with the uniform refinement. For both error estimators, the maximum error of the adaptive grids is lower than for the uniform grid case. The final adaptive grid has a maximum error 10 times much lower than for the case of the uniform grid.

In this case, the error slope is not always constant due to the grid interface correction, which prevents the accumulation of the grid interfaces between different levels of

refinement, avoiding the loss of the grid quality and the solution overall accuracy.

When comparing the results from the subfigure 6(b) with the ones obtained by Jasak and Gosman [5] there is a significant improvement. This happens due to the grid interface correction and the different decision algorithm of the cells for refinement.

4.3 Flow over a Sphere

The three dimension flow over a sphere is computed as the final test of the RLS estimator and the adaptive code, two initial meshes were made one with hexahedrons and another one with tetrahedrons. The initial hexahedron grid has 46800 cells and its domain has a cylinder form, the computational domain of the initial tetrahedral grid is a squared prism with $39 \times 13 \times 13$ diameters and has 126182 cells.

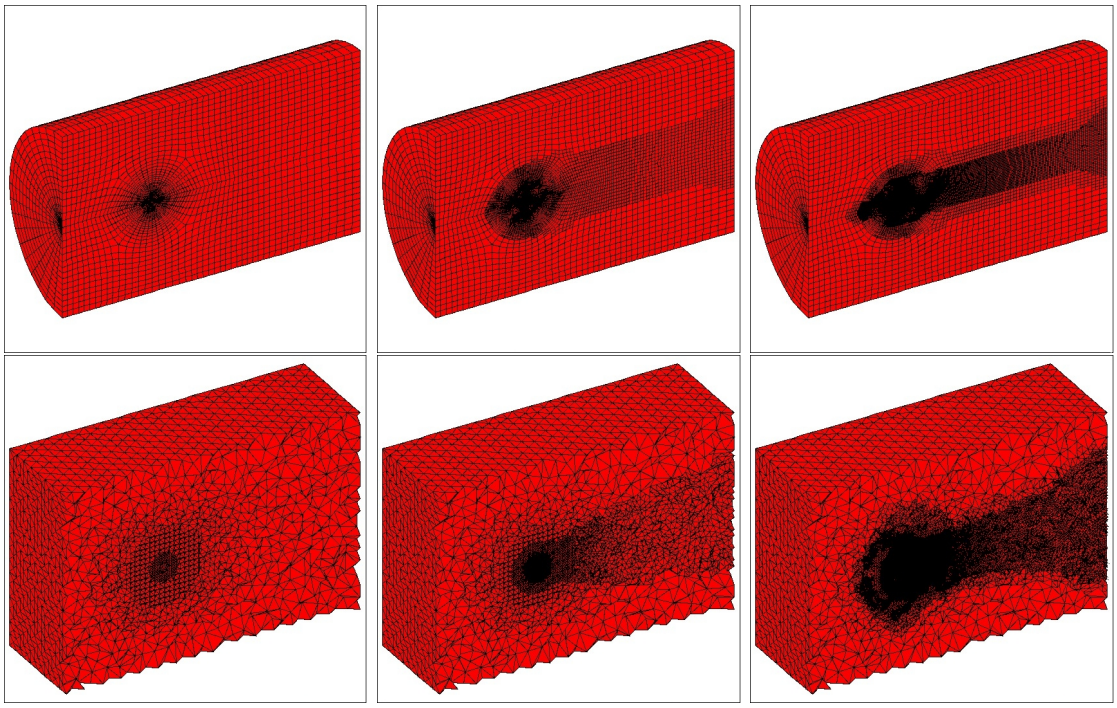

Figure 7: Example of Refinement in the Sphere Flow with Hexahedral and Tetrahedral Grids

Figure 7 shows the adaptive grids for two levels of refinement, with both the hexahedral and tetrahedral grids, for a Reynolds number of 200. The final meshes have 1331216 and 2707026 cells, respectively, which corresponds to a mesh with less 55.555% and 66.479% than compared to uniform refinement case. Both adaptive grids are refined near the sphere wall and in the flow's wake which are the primary features of this problem. The cone formed by the refined cells in the flow's wake is bigger in the tetrahedral grid, since the cells far away of the sphere have a higher hydraulic radius than in the hexahedral grid.

5 CONCLUSIONS

- The Residual Least Squares (RLS) error estimator has been shown to be suitable for adaptive refinement of Finite-Volume methods on unstructured grids. Unlike other error estimators, the RLS has information of the governing equations discretization and information of the grid quality.

- The new adaptive decision algorithm is independent on user defined parameters and can deal with the problem of the grid quality loss in the cell interface, making it more suitable than other algorithms from the literature.

ACKNOWLEDGMENTS

The first author would like to thank the support received by the Portuguese FCT (Foundation for Science and Techology) grant SFRH/BD/48150/2008.

REFERENCES

[1] J. P. Magalhães, J. M. C. Pereira, and J. C. F. Pereira. A new refinement criterion based on regression diagnostics for finite volume methods. *Int. Conf. on Adaptive Modeling and Simulation (ADMOS), Goteborg*, 2007.

[2] D. M. S. Albuquerque, J. M. C. Pereira, and J. C. F. Pereira. Refinement least squares regression criteria applied to laminar flows. *Int. Conf. on Adaptive Modeling and Simulation (ADMOS), Paris*, 2011.

[3] J. P. Magalhães, D. M. S. Albuquerque, J. M. C. Pereira, and J. C. F. Pereira. Adaptive mesh finite-volume calculation of 2d lid-cavity corner vortices. *J. Comp Phys., Accepted for Publication*, 2013.

[4] H. Jasak and A. D. Gosman. Automatic resolution control for the finite volume method, part 1: A-posteriori error estimates. *Numer. Heat Transfer, Part B*, 38(3):237–56, 2000.

[5] H. Jasak and A. D. Gosman. Automatic resolution control for the finite volume method, part 2: Adaptive mesh refinement and coarsening. *Numer. Heat Transfer, Part B*, 38(3):257–71, 2000.

[6] M. Ainsworth and J. T. Oden. A posteriori error estimation in finite element analysis. *Comput. Methods Appl. Mech. Eng.*, 141:1–88, 1997.

[7] K. J. Fidkowski and D. L. Darmofal. Review of output-based error estimation and mesh adaptation in computational fluid dynamics. *AIAA Journal*, 49(4):673–694, 2011.

[8] T. Gratsch and K. Bathe. A posteriori error estimation techniques in practical finite element analysis. *Computers and Structures*, 83:235–265, 2005.

[9] K. Segeth. A review of some a posteriori error estimates for adaptive finite element methods. *Mathematics and Computers in Simulation*, 80:1589–1600, 2008.

[10] M. J. Berger and J. Oliger. Adaptive mesh refinement hyperbolic partial differential equations. *J. Comp Phys.*, 53:484–512, 1984.

[11] D. C. Haworth, E. L. Thary, and M. S. Huebler. A global approach to error estimation and physical diagnostics in multidimensional fluid dynamics. *Int. J. Numer. Meth. Fluids*, 17:75–97, 1993.

[12] S. Muzaferija and D. Gosman. Finite-volume CFD procedure and adaptive error control strategy for grids of arbitrary topology. *J. Comp Phys.*, 138:766–787, 1997.

[13] Djaffar Ait-Ali-Yahia, Guido Baruzzi, Wagdi G. Habashi, Michel Fortin, Julien Dompierre, and Marie Gabrielle Vallet. Anisotropic mesh adaptation: towards user-independent, mesh-independent and solver-independent CFD. part i: general principles. *International Journal of Numerical Methods in Fluids*, 32(6):725–744, 2002.

[14] H. Jasak and A. D. Gosman. Residual error estimate for the finite-volume method. *Numer. Heat Transfer, Part B*, 39(1):1–19, 2001.

[15] F. Juretic. Error analysis in finite volume CFD. *PhD thesis, Imperial College, University of London*, 2004.

[16] S. V. Patankar and D. B. Spalding. A calculation procedure for heat, mass and momentum transfer in three dimensional parabolic flows. *Int. Journal Heat and Mass Transfer*, 15:1787, 1972.

[17] C. M. Rhie and W. L. Chow. Numerical study of the turbulent flow past an airfoil with trailing edge separation. *AIAA Journal*, 21:1525–1532, 1983.

[18] M. Kobayashi, J. M. C. Pereira, and J. C. F. Pereira. A second-order upwind least-squares scheme for incompressible flows on unstructured hybrid grids. *Num. Heat Transfer B*, 34:39–60, 1998.

[19] M. Kobayashi, J. M. C. Pereira, and J. C. F. Pereira. A conservative Finite-Volume second-order accurate projection method on hybrid unstructured grids. *J. Comp. Phys.*, 150:40–75, 1999.

[20] J. H. Ferziger and M. Peric. *Computational method for Fluid Dynamics*. Springer-Verlag, Berlin/New York, 1996.